

The DAMPE Silicon-Tungsten Tracker

P. Azzarello^{a,*}, G. Ambrosi^b, R. Asfandiyarov^a, P. Bernardini^{c,d}, B. Bertucci^{b,e},
A. Bolognini^{b,e}, F. Cadoux^a, M. Caprai^b, I. De Mitri^{c,d}, M. Domenjoz^a,
Y. Dong^f, M. Duranti^{b,e}, R. Fan^f, P. Fusco^{g,h}, V. Gallo^a, F. Gargano^g, K. Gong^f,
D. Guo^f, C. Husi^a, M. Ionica^{b,e}, D. La Marra^a, F. Loparco^{g,h}, G. Marsella^{c,d},
M. N. Mazziotta^g, J. Mesa^a, A. Nardinocchi^{b,e}, L. Nicola^a, G. Pelleriti^a,
W. Peng^f, M. Pohl^a, V. Postolache^b, R. Qiao^f, A. Surdo^d, A. Tykhonov^a,
S. Vitillo^a, H. Wang^f, M. Weber^a, D. Wu^f, X. Wu^a, F. Zhang^f

^a*Département de Physique Nucléaire et Corpusculaire, University of Geneva, Geneva, Switzerland*

^b*Istituto Nazionale di Fisica Nucleare Sezione di Perugia, Perugia, Italy*

^c*Dipartimento di Matematica e Fisica "E. De Giorgi", Univerisità del Salento, Lecce, Italy*

^d*Istituto Nazionale di Fisica Nucleare Sezione di Lecce, Lecce, Italy*

^e*Dipartimento di Fisica e Geologia, Univerisità di Perugia, Perugia, Italy*

^f*Institute of High Energy Physics, Chinese Academy of Sciences, Beijing, China*

^g*Istituto Nazionale di Fisica Nucleare Sezione di Bari, Bari, Italy*

^h*Dipartimento di Fisica "M. Merlin" dell'Univerisità e del Politecnico di Bari, Bari, Italy*

Abstract

The DARK Matter Particle Explorer (DAMPE) is a spaceborne astroparticle physics experiment, launched on 17 December 2015. DAMPE will identify possible dark matter signatures by detecting electrons and photons in the 5 GeV - 10 TeV energy range. It will also measure the flux of nuclei up to 100 TeV, for the study of the high energy cosmic ray origin and propagation mechanisms. DAMPE is composed of four sub-detectors: a plastic strip scintillator, a silicon-tungsten tracker-converter (STK), a BGO imaging calorimeter and a neutron detector. The STK is composed of six tracking planes of 2 orthogonal layers of single-sided micro-strip detectors, for a total detector surface of ca. 7 m². The STK has been extensively tested for space qualification. Also, numerous beam tests at CERN have been done to study particle detection at silicon module level, and at full detector level. After description of the DAMPE payload and its scientific mission, we will describe the STK characteristics and assembly. We will then focus on some results of single ladder performance tests done with particle beams at CERN.

*Corresponding author

Preprint submitted to *Physics Letters B* on February 11, 2016

20 **1. Introduction**

21 The DARK Matter Particle Explorer (DAMPE) is a high energy astroparticle
22 physics satellite. It is one of the five space science missions of the “Strategic
23 Pioneer Program on Space Science” [1] of the Chinese Academy of Sciences
24 (CAS).

25 The scientific goals of DAMPE is to measure precisely the summed spectrum
26 of electrons and positrons, and the photon spectrum between 5 GeV to 10 TeV,
27 as well as the cosmic ray flux and chemical composition from 10 GeV to above
28 100 TeV. The geometrical acceptance is of $\sim 0.3 \text{ m}^2\text{sr}$, for electrons and photons,
29 $\sim 0.2 \text{ m}^2\text{sr}$ for cosmic rays. To achieve this, a thick total absorption calorimeter
30 is combined with a precise tracker equipped with integrated photon converter .

31 The DAMPE detector (figure 1) is composed of four sub-detectors. The
32 plastic scintillator strip detector (PSD) is composed of one double-layer (one x
33 and one y) of scintillating strips. It serves as anti-coincidence detector for photon
34 identification, as well as a charge detector for the cosmic rays. The second sub-
35 detector is the Silicon-Tungsten Tracker (STK) and will be discussed in detail
36 in the following sections. The third sub-detector, the calorimeter, is made up
37 of 14 layers of BGO bars in a hodoscopic arrangement. The total thickness
38 of the calorimeter is equivalent to 31 radiation lengths, and 1.6 interaction
39 lengths. The last sub-detector is the neutron detector (NUD). It is made of
40 16 1-cm thick boron-doped plastic scintillator plates. The purpose of the NUD
41 is to detect delayed neutrons resulting from a hadron shower, to improve the
42 electron/photon separation power, expected to be 10^5 overall.

43 Design, prototyping, production, test and qualification of DAMPE payload
44 has been carried out by collaborating institutes of China, Switzerland and Italy.

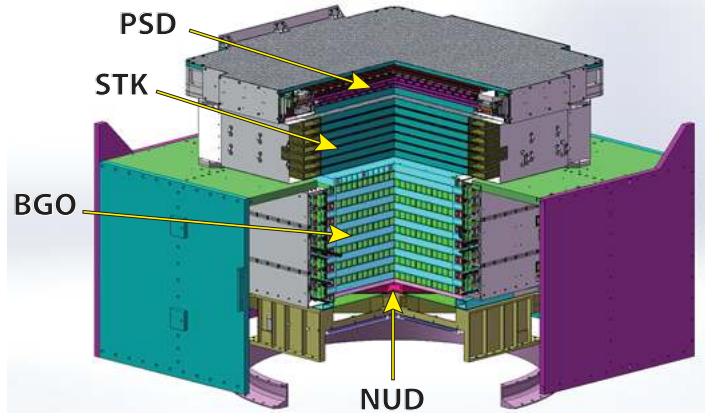


Figure 1: The DAMPE satellite payload. It is composed of a plastic strip scintillator (PSD), a silicon-tungsten tracker (STK), a BGO calorimeter, and a neutron detector (NUD).

45 2. The Silicon-Tungsten Tracker (STK)

46 The principle of the STK is based on an approach used in previous space
 47 experiments (Fermi[2], Agile [3]). Incoming photons convert to an electron-
 48 positron pair in one of the tungsten converters. The pair is then detected in
 49 the subsequent silicon layers. Multiple scattering of charged particles can be
 50 reduced by spreading the tungsten to several foils. For high energy particles
 51 (>5 GeV), the effect is negligible if the tungsten thickness is of a few millimeters
 52 ($\theta_0 = 0.08^\circ$ for 1 mm tungsten, and 5 GeV particles).

53 The STK is made of 6 tracking planes each consisting of two layers of single-
 54 sided silicon micro-strip detectors measuring the two orthogonal views perpen-
 55 dicular to the pointing direction of the detector. Three layers of tungsten plates
 56 of 1 mm thickness are inserted in front of tracking layers 2, 3 and 4, for photon
 57 conversion. Tracking layer 1 provides the coordinate of the entrance point of the
 58 passing particle, to be linked with the measurement of the PSD sub-detector.
 59 The absence of tungsten after tracking layer 4 allow to cleanly reconstruct the
 60 track of electron-positron pairs produced by photon conversion in the last tung-
 61 sten layer.

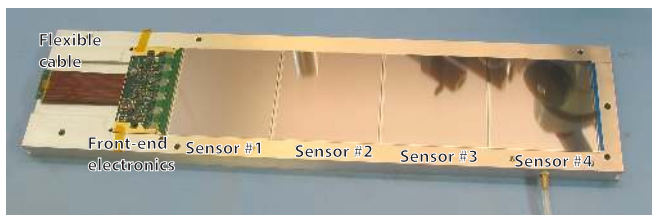


Figure 2: The silicon ladder is made of four silicon micro-strip detectors. The front-end electronics is located at one extremity of the ladder. It reads out 384 strips, with a readout pitch of $242\ \mu\text{m}$. Six VA140 ASICs are used for the signal amplification.

62 *2.1. The silicon detector module*

63 The DAMPE STK is composed of 192 silicon modules, named ladders, made
 64 of 4 single-sided micro-strip detectors (figure 2). The sensor strips are parallel
 65 to the ladder length, and are daisy-chained via micro-wire bonds.

66 The silicon detectors, manufactured by Hamamatsu Photonics [4], consists
 67 of 768 p^+ -strips implanted in the n-doped bulk. The strips are AC-coupled
 68 and biased through polysilicon resistors. The dimensions of the detectors is
 69 $95 \times 95 \times 0.32\ \text{mm}^3$. The detector is essentially the same as the one used in
 70 AGILE [3], except for the thickness, bulk resistivity and backside metallization
 71 (gold instead of aluminum, to improve backside contact). The bulk resistivity is
 72 $> 7\ \text{k}\Omega \cdot \text{cm}$, thus the full depletion voltage is 50 V at maximum. The strips are
 73 $48\ \mu\text{m}$ wide and 93.196 mm long, with a pitch of $121\ \mu\text{m}$. The typical coupling
 74 capacitor value is 500 pF, and polysilicon resistors are typically of 35 M Ω . Over
 75 the full silicon sensor production the average total leakage current is of 116 nA
 76 at 150 V, well below the specification of 900 nA.

77 To limit power consumption, electronics density and transferred data, every
 78 other strip is readout, thus one ladder provides a total of 384 readout channels.
 79 The ladders are operated with a bias voltage of 80V.

80 *2.2. Front-end electronics and data acquisition*

81 The Tracker Front-end Hybrid (TFH) board collects and amplifies the signals
 82 coming from the strips. Mechanically it is also an important component of the

1083 ladder, as the detectors are glued on the 380mm-long flex extension of the
1084 board. Through the flex part, the TFH brings the bias voltage to the backside
1085 of the detectors. For redundancy two DS18S20 temperature sensors [5] are
1086 also mounted on the TFH. The board also integrates a flexible cable for the
1087 connection to the DAQ boards (figure 2).

1088 The ASIC used for the strip signal shaping and amplification is the VA140,
1089 produced by IDEAS [6]. The VA140 is a 64 channel low-noise/low power high
1090 dynamic range charge sensitive preamplifier-shaper circuit, with simultaneous
1091 sample and hold, multiplexed analog readout, calibration facilities and internally
1092 generated biases. The VA chip family is a well-known component, already used
1093 in astroparticle physics experiments like AMS-01 and AMS-02 [7], where they
1094 have been used for the readout of the double-sided micro-strip detectors of the
1095 tracker. The power consumption of one ladder is 116 mW.

1096 *2.3. Silicon ladder assembly*

1097 The ladder assembly consists of the front-end board glued onto the four sil-
1098 icon detectors, initially placed on a precision alignment jig. After gluing, the
1099 position of the silicon detectors is measured with a coordinate measurement ma-
1100 chine. A linear fit is applied to the measured positions of the detector alignment
1101 patterns. The RMS of the residual distribution is then computed, to estimate
1102 the alignment error. Figure 3 shows the average alignment error of the 192 lad-
1103 ders installed on the STK. Thanks to the jigs, the alignment precision is about
1104 $4\ \mu\text{m}$ on average, much better than the required $40\ \mu\text{m}$.

1105 Part of the ladder quality assurance, a 12-hour cosmic ray test is performed
1106 and the signal to noise ratio of cluster charges from minimum ionizing particle
1107 (MIP) is checked. On average the S/N is about 15, excellent for the application
1108 of the STK. All 192 ladders needed for the STK Flight Model were produced
1109 by the end of March 2015, for a total production time of three months, shared
1110 between two production sites (University of Geneva and INFN Perugia). The
1111 silicon detector quality has been preserved during all the STK assembly steps,
1112 the 192 ladder leakage current at 80V is 330 nA in average (figure 4).

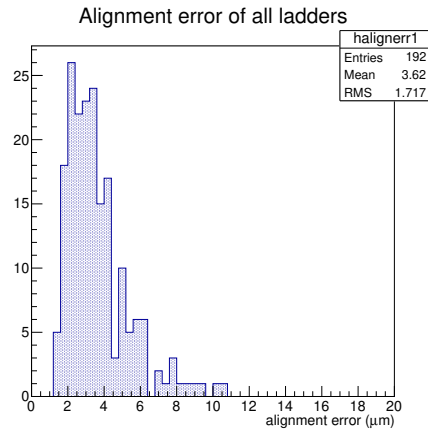


Figure 3: Alignment error of the 192 ladders mounted on the STK. The average alignment error is less than 4 μm , much better than the required 40 μm .

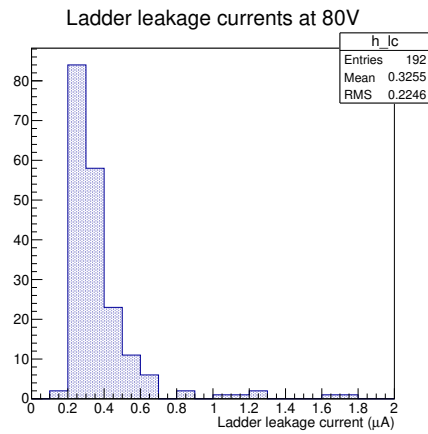


Figure 4: Total leakage current at 80V bias of the 192 ladders of the flight model STK. The average current is 330 nA, which means that the silicon detector quality has been preserved during the ladder assembly.

113 *2.4. Plane assembly*

114 The 192 ladders are distributed on seven support trays. Five are equipped
115 on both sides, while the front and the rear trays are equipped only on the side
116 facing the interior of the tracker. A layer is composed of 16 ladders, arranged
117 in two rows of eight. A layer is thus composed of an array of 8×8 detectors, as
118 can be seen on figure 5. On the double-sided trays, the silicon layer strips are
119 orthogonal to each other.

120 A support tray is made of an aluminum honeycomb structure sandwiched
121 between two Carbon Fibre Reinforced Polymer (CFRP) face sheets of 0.6 mm
122 thick each (1.0 mm for trays with tungsten). It forms a light but rigid structure
123 that can sustain the vibrations and the accelerations of a rocket launch. For the
124 second, third and fourth trays, 1 mm thick tungsten plates are glued onto the
125 lower CFRP sheet, inside the tray. The converter is thus located immediately
126 above the corresponding tracking layer, to ensure good efficiency of conversion
127 detection. The trays have been produced at Composite Design Sàrl [8]. The
128 trays equipped with tungsten layer have been X-ray scanned at CERN, to check
129 the alignment of the tungsten plates with respect to the four tray corners.

130 The ladder installation on each tracker tray has been done using an alignment
131 and transfer jig, placed onto a precision frame holding the tray. The position
132 of the 64 silicon sensors of the fully equipped tray were then measured with a
133 coordinate measurement machine.

134 The trays have been stacked on top of each other to form the full tracker
135 (figure 5). The silicon ladders on the bottom surface of a tracker tray and those
136 on the top surface of the tray below form an X-Y tracking plane, the distance
137 between the X and the Y layer of a tracking plane is ~ 3 mm. The stack of the
138 7 trays forms 6 tracking planes that provide 12 measurement points (6 X and 6
139 Y) when a charged track traverses the STK.

140 The STK has a total power consumption of 90 W. The tracker cooling is
141 ensured with a network of heat conductors. Pyrolytic graphite sheets (PGS)
142 connect the front-end lateral sides with a horizontal copper band installed on
143 the tray edges. Copper straps are transversely glued to thermally connect the



Figure 5: The STK before the assembly of the last tray. The 64 silicon detectors are visible, together with the horizontal copper bands used for the heat transfer.

144 trays together, and to the aluminum radiators placed on the four lateral sides
145 of the STK. During installation on the satellite, heat pipes have then been
146 mounted, to ensure a constant radiator temperature of 10 C.

147 **3. Signal digitization and readout**

148 The VA chips are separated into two independent readout groups (VAs 1
149 to 3, and VAs 4 to 6). Both groups are readout in parallel, but the VAs of a
150 same group are serially readout. Thus 192 clock signals are necessary to transfer
151 the 384 silicon strip signals. Each group has its own amplification circuit, which
152 analogical outputs are then transferred to the main STK data acquisition boards
153 (Tracker Readout Boards, TRB).

154 A TRB circuit reads out 24 ladders, and is composed of a stack of three
155 boards. The ADC board, to which are connected the ladders, performs the
156 analog to digital conversion of the ladder signals. The FPGA board has two
157 FPGAs which manage the communication with the DAMPE DAQ system, and
158 the generation of the control signals necessary for the 24 ladder readout and
159 signal digitization. The Power board produces the voltages necessary for the
160 front-end electronics and the TRB circuit, as well as the silicon bias voltages.
161 To reduce the data size, the FPGAs perform a data compression, using a zero-
162 suppression and cluster finding algorithm. Eight TRBs are needed to readout
163 the whole STK: two TRBs are mounted side by side on each STK edge. The
164 TRB system has been designed and produced by IHEP, Beijing.

165 4. Silicon detector performance studies

166 DAMPE will not only measure ionization by singly-charged particles but also
167 nuclei. The study of cosmic ray propagation models are tested by examining the
168 abundance ratios of secondary to primary particles, such as boron to carbon.
169 For this it is necessary to record the amplitude of the signal measured at the
170 strip level, and to precisely reconstruct the charge deposited inside the silicon
171 detectors. Such study has to be conducted in two steps, first with particles of
172 charge 1, then with higher charge particle. The next sections will focus on tests
173 done with charge 1 particles.

174 As the strip analog signal is acquired, it is also interesting to evaluate the
175 position resolution performance of the detector, in terms of particle track impact
176 point and incidence angle.

177 For these purposes two modules have been exposed to 400 GeV proton beams
178 at CERN. The ladders were installed in the middle of a beam telescope made
179 of six HV-CMOS pixel detectors built by the ATLAS Geneva group, providing
180 track resolution of $\sim 5 \mu\text{m}$. The module performance in terms of charge collection
181 and spatial resolution for different angle of incidence have been studied.

182 4.1. Performance for 0° incident angle

183 A cluster finding is done on each event, after pedestal and common mode
184 noise subtraction. A cluster is by definition a group of at least one channel
185 having a signal larger than 4 times the channel noise, and having all neighboring
186 channels with signal larger than 1.5 the channel noise. The cluster charge is then
187 the sum of each individual channel signal, in ADC counts. Each channel signal,
188 measured in ADC counts, is proportional to the electrical charge measured at
189 the input of the VA channel. If no charge is lost inside the silicon detector, the
190 cluster charge is proportional to the energy deposited by the traversing particle.

191 The typical cluster charge distribution for particles with 0° incidence is
192 shown in figure 6. One clearly notes the double-peak structure of the distri-
193 bution. This is due to the contribution of two separate distributions. The one

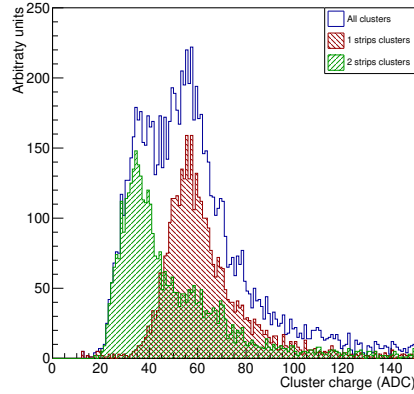


Figure 6: Signal distribution for a DAMPE silicon ladder, for charge one particles. Two distributions are clearly visible. The highest peak distribution corresponds to the contribution of the single-channel clusters, while the lowest peak distribution corresponds to the 2-channel clusters.

194 with largest maximum is due to the contribution of particles traversing the de-
 195 tector close to a readout strip. In such cases the cluster is mostly composed
 196 of a single channel. The distribution with lower maximum is the contribution
 197 from the particles traversing the detector close to floating strips, i.e. strips
 198 which are not connected to the front-end electronics, thus generating a 2-strips
 199 cluster. When the particle travels close to a floating strip, the electrical signal
 200 generated by ionization is then shared with the two neighbors connected to the
 201 front-end, through capacitive coupling. Depending on the capacitive properties
 202 of the strips between each other, and with the detector bulk, part of the charge
 203 will not reach the readout strips. In the case of the DAMPE ladders, $\sim 65\%$ of
 204 the originally generated charge is actually measured by the neighboring readout
 205 strips, as we can see in figure 6.

206 Such an effect must be then taken into account when one needs to precisely
 207 measure the energy deposited by the crossing particle.

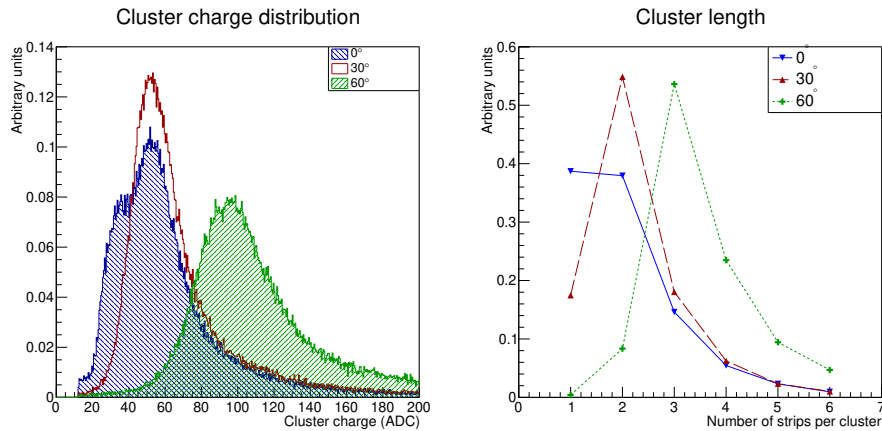


Figure 7: Cluster charge distribution (left) and cluster size (right) for incident angles 0° , 30° and 60° .

208 4.2. Performance for inclined tracks

209 In DAMPE, the maximum incidence angle acceptance of the STK is limited
 210 by the size of BGO to 60° . It is thus interesting to study the detector behavior
 211 for inclined tracks. The rotation axis considered here is parallel to the strips,
 212 to study the cluster size change with respect to the particle incidence angle.
 213 Thanks to the high resolution beam telescope, the reconstructed tracks allows
 214 for a detailed study of the charge collected by the detector for various incidence
 215 angles. Data within a range from 0° to 70° , with a step of 10° have been
 216 collected. The figure 7 (left) shows the cluster charge distributions for three
 217 angles of incidence (0° , 30° and 60°).

218 When the track is inclined, the charge collected at the level of the readout
 219 strips is the result of two contributions. In addition to the effects of the capac-
 220 itive charge sharing observed for the 0° -angle tracks (figure 6), the inclination
 221 of the track induces a charge distribution between all the strips covered by the
 222 projection of the track on the silicon plane. As an example, with an incident
 223 angle of 21° , the projected track covers a distance equivalent to the strip pitch
 224 p of $121\ \mu\text{m}$: the charge will be shared between two neighboring strips. For
 225 the typical study angles of 30° and 60° , the projected distance is equivalent to

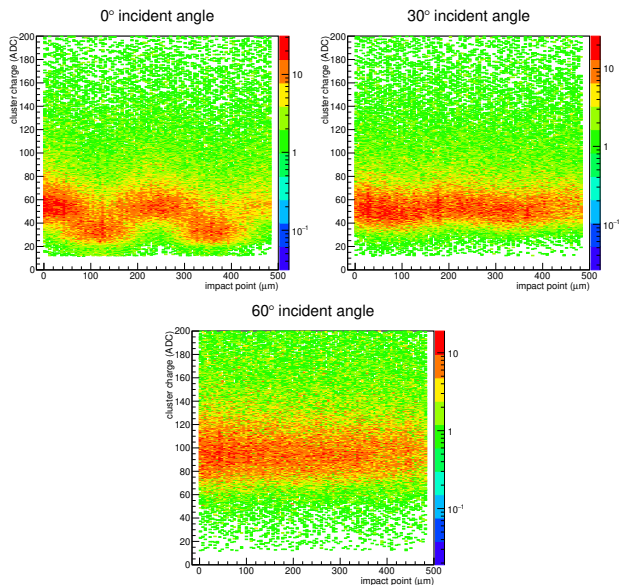


Figure 8: Measured energy as a function of the impact point, for 0° , 30° and 60° incident angles. The effect of different charge collection behavior, visible at 0° , is already much attenuated at 30° .

226 $1.5 \cdot p$ and $4.6 \cdot p$, respectively. As an example, the cluster size for three different
 227 angles of incidence is shown in figure 7 (right). As expected, for 30° , the charge
 228 is mainly shared between two readout strips, while the number of involved strips
 229 increases to three at 60° .

230 Defining as impact point (IP) the position of the track on the silicon ladder
 231 as extrapolated by the beam telescope, we examined the cluster charge as a
 232 function of the impact point and the incident angle (figure 8). While at 0° one
 233 can clearly see the effect of different charge collection depending on the passage
 234 close to a readout or floating strip, this effect attenuates when the incidence
 235 angle increases, as more strips are involved in the charge detection.

236 5. Spatial resolution

237 Defining the cluster center of gravity (*cog*) as the weighted mean of the
 238 position of each strip, we define the residual r as: $r = IP - cog$. Figure

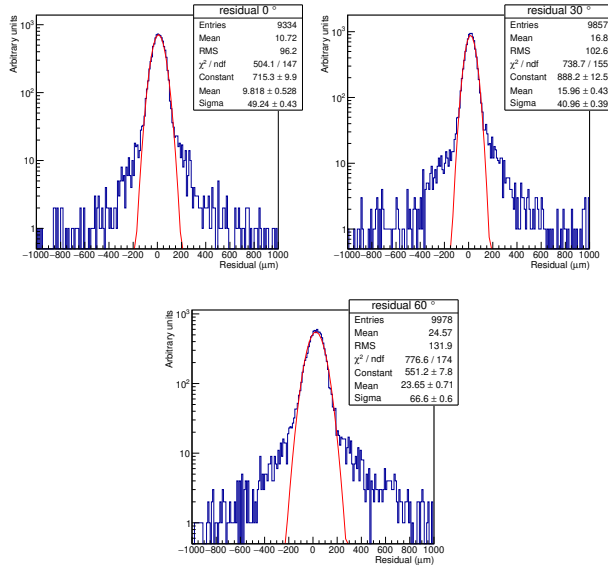


Figure 9: Residual distributions, for 0°, 30° and 60° incident angles. The σ of the gaussian fit provides a preliminary estimation of the detector spatial resolution.

239 9 shows the gaussian fits of the residual distributions for incidence angles of
 240 0°, 30° and 60°. The resolution can thus be extrapolated from the σ of the
 241 gaussian fit (the contributions due to the resolution of the beam telescope are
 242 negligible). The results shown in figure 9 are still preliminary and a detailed
 243 study of the dependence on impact point and cluster dimension is in progress.
 244 Figure 10 shows the resolution from 0° to 70° in steps of 10°. Thanks to the
 245 analog readout, it is possible to take into account the charge sharing due to the
 246 capacitive strip coupling. The resolution is less than 50 μm for incidence angles
 247 lower than 40°, and always much lower than the 70 μm achieved with a digital
 248 position finding algorithm [9].

249 6. Status of STK Flight Model

250 The STK Flight Model, to be used in the DAMPE payload, has been inte-
 251 grated in April 2015 in Geneva and tested with cosmic rays for several days,
 252 before being delivered to IHEP in Beijing. Acceptance level of vibration and

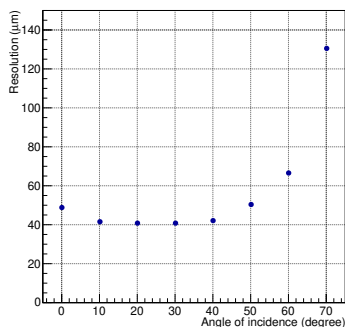


Figure 10: Spatial resolution as a function of the impact angle. Below 70° , the resolution is much lower than the $70\mu\text{m}$ achieved with a digital position finding algorithm.

253 thermal vacuum tests were conducted in Beijing in May 2015. In June 2015
 254 the STK Flight Model has successfully passed the DAMPE payload integration
 255 test, then the DAMPE satellite integration test. In July 2015 the full DAMPE
 256 instrument has been tested in a thermal vacuum chamber. A vibration test
 257 was done in September 2015, followed by in flight simulation tests and aging
 258 tests. After 6 months of intensive manipulations and tests, the STK remains
 259 in excellent quality: as of November 2015, the number of noisy channels (noise
 260 > 5 ADC counts) is stable since the STK integration and remains below 0.5%.
 261 Only 18 ($< 0.03\%$) channels out of the 74382 need to be masked. The DAMPE
 262 satellite has been transferred to the launch site on Nov. 15th, 2015.

263 7. Conclusions

264 The Silicon-Tungsten tracker (STK) of the DAMPE mission is based on the
 265 robust technology of single-sided micro-strip detectors with analog readout. It
 266 will play a crucial role in track reconstruction, gamma-ray detection, cosmic
 267 ray charge measurement and overall particle identification. The flight model
 268 has been assembled from January to April 2015, then delivered to China, where
 269 it has successfully passed all the acceptance tests. The silicon modules are
 270 thoroughly studied, and measurements done for individual modules to calibrate

271 the full STK. The charge collection in terms of particle impact point and angle
272 have been presented. Thanks to the analog readout of the strips, it is possible
273 to evaluate the incoming particle charge, as well as achieve a spacial resolution
274 better than 50 μm , for incident angles lower than 40°.

275 The DAMPE satellite has been assembled during the summer 2015, and has
276 been successfully launched on 17 December 2015.

277 **Acknowledgement**

278 The authors wish to express their gratitude to M. Prest and E. Vallazza of
279 the AGILE Silicon Tracker collaboration for fruitful discussions on tracker de-
280 sign and for kindly allowing us to use the AGILE silicon sensor geometry. The
281 generosity of CERN for providing beam time allocation and technical assistance
282 at the PS and SPS beam lines, as well as general logistical support is acknowl-
283 edged. This work is supported by the Chinese Academy of Sciences, the Swiss
284 National Science Foundation and INFN, Italy.

285 **References**

- 286 [1] Science Magazine 332 (6032) 904.
- 287 [2] W. B. Atwood et al., The Astrophysical Journal 697 (2) (2009) 1071.
- 288 [3] M. Feroci et al., Nucl. Instr. and Meth. A 581 (2007) 728–754.
- 289 [4] <http://www.hamamatsu.com>.
- 290 [5] <https://datasheets.maximintegrated.com/en/ds/DS18S20.pdf>.
- 291 [6] Integrated Detector Electronics AS, <http://www.ideas.no>.
- 292 [7] G. Ambrosi, Nucl. Instr. and Meth. A 435 (1999) 215–223.
- 293 [8] <http://www.compositedesign.ch>.
- 294 [9] R. Turchetta, Nucl. Instr. and Meth. A 335 (1993) 44–58.